Supplementary Information for:

Simultaneously Detection and Removal of Organophosphorus Pesticide by A novel Zr-MOF based Smart Adsorbent

Qingfeng Yang[a], Jing Wang[a], Xinyu Chen[a], Weixia Yang[a], Hanna Pei[a], Na Hu[b], Zhonghong Li[a], Yourui Suo[b], Tao Li[c], Jianlong Wang[a,*]

[a] College of Food Science and Engineering, Northwest A&F University, Yangling, 712100, Shaanxi, China.

[b] Qinghai Key Laboratory of Qinghai-Tibet Plateau Biological Resources，Northwest Institute of Plateau Biology, Chinese Academy of Sciences, Xining, Qinghai, 810008, China.

[c] Shaanxi Institute for Food and Drug Control, Xi'an, 710065, China

* Corresponding author.

E-mail address: wanglong79@yahoo.com (Jianlong Wang)

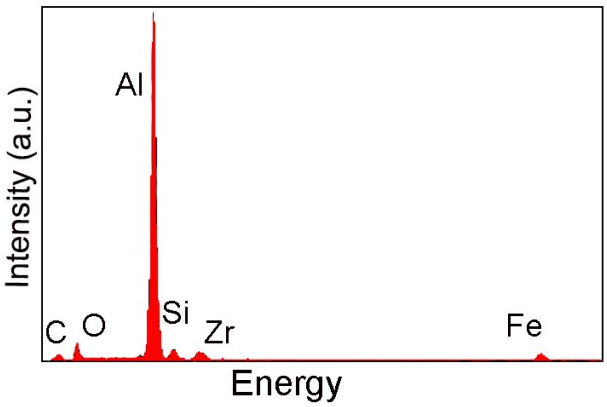

Fig. S1 The EDX spectrum of the Fe_3O_4@SiO_2@UiO-67.

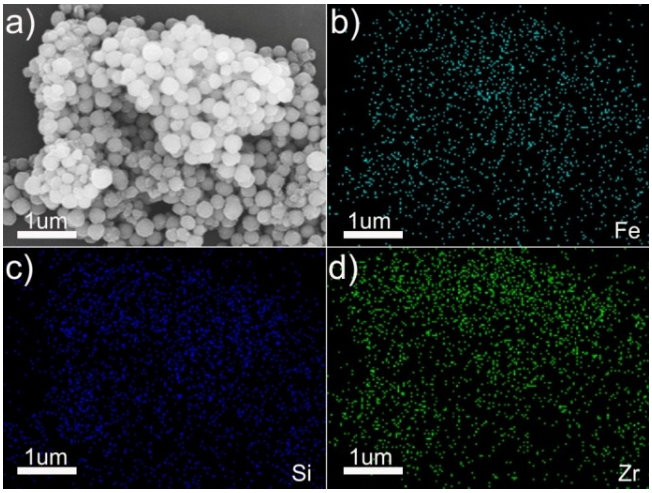

Fig. S2 The elemental mapping of Fe_3O_4@SiO_2@UiO-67 including Fe (b), Si (c), and Zr (d) elements.

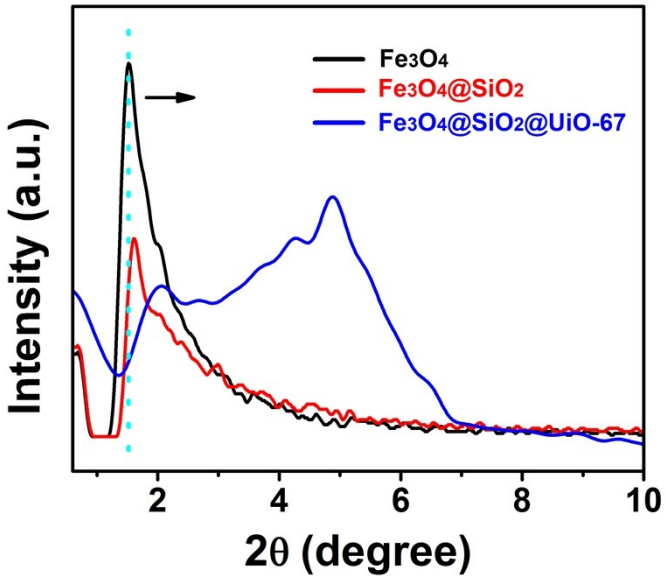

Fig. S3 Small-angle X-ray diffraction of Fe_3O_4, $Fe_3O_4@SiO_2$, and $Fe_3O_4@SiO_2@UiO\text{-}67$.

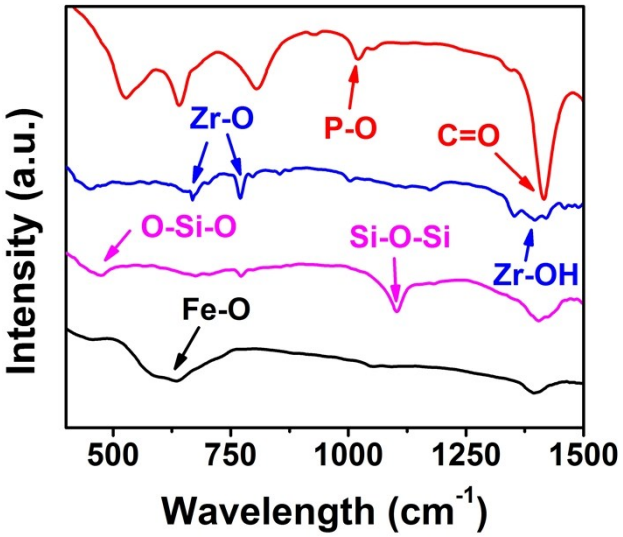

Fig. S4 The FTIR spectra of Fe_3O_4 (black line), Fe_3O_4@SiO_2 (pink line), Fe_3O_4@SiO_2@UiO-67 before and after adsorption of glyphosate (blue and red line) in the range of 400 to 1500 cm^{-1}.

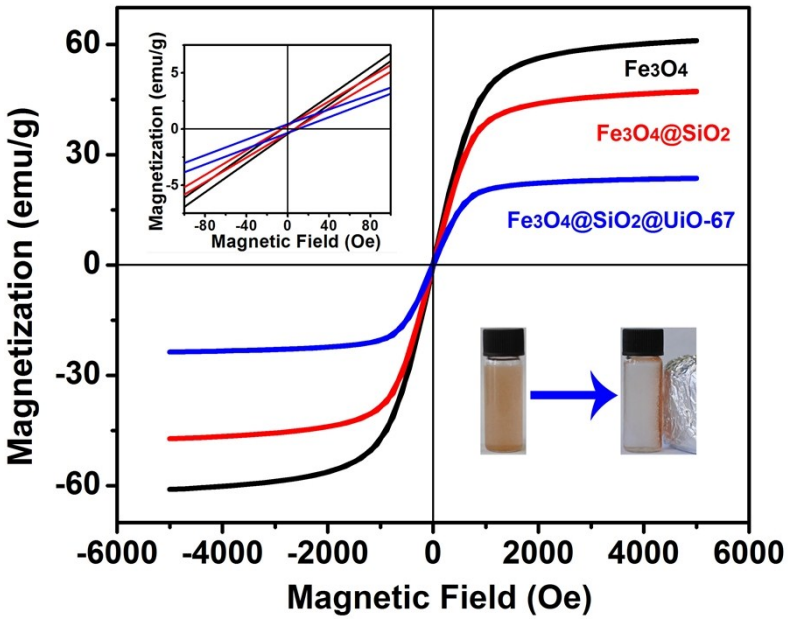

Fig. S5 Hysteresis loops of Fe_3O_4, Fe_3O_4@SiO_2, and Fe_3O_4@SiO_2@UiO-67 (Left inset: low-magnetic field region of hysteresis loops; Right inset: the photographic images of Fe_3O_4@SiO_2@UiO-67 before and after magnetic separation).

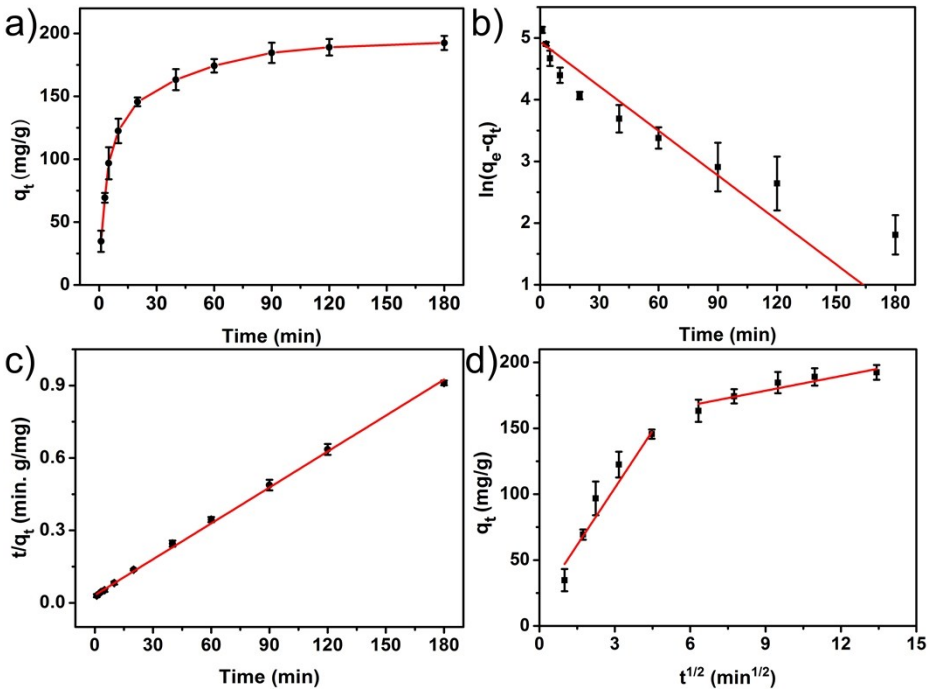

Fig. S6 (a) The effect of contact time on glyphosate adsorption. The plots of different model including pseudo-first-order kinetic (b), pseudo-second-order kinetic (c), and intraparticle diffusion kinetic (d).

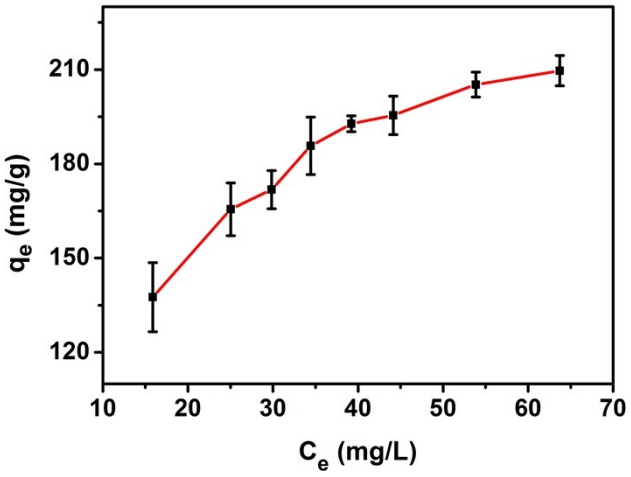

Fig. S7 The influence of initial concentration of glyphosate on adsorption capacity.

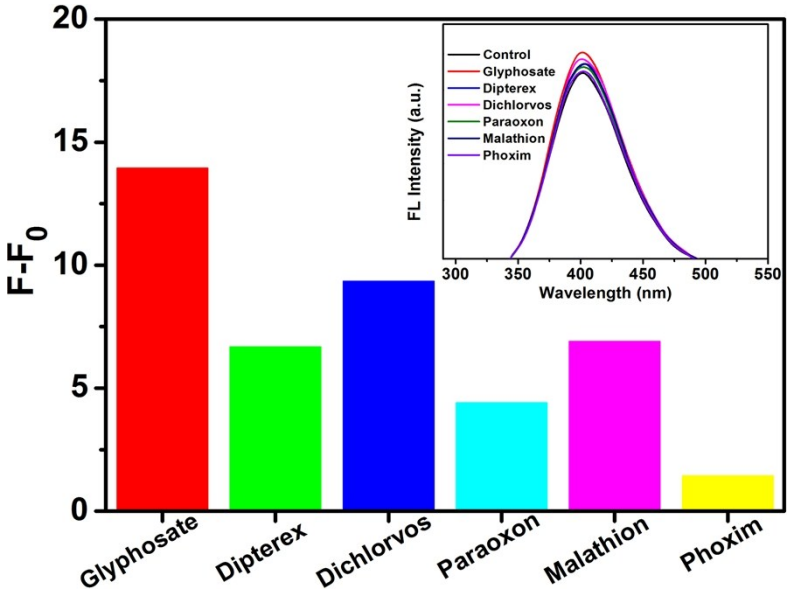

Fig. S8 The effect of different OPPs in detection of glyphosate.

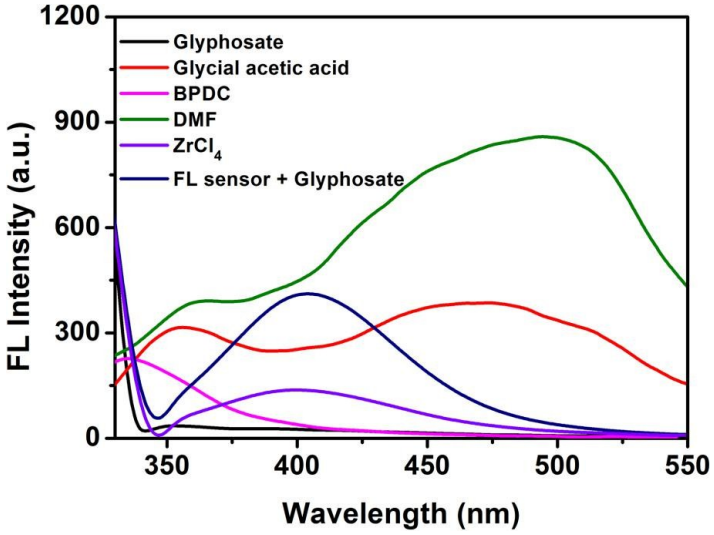

Fig. S9 The emission spectra of different individual precursors of UiO-67 and after addition of glyphosate.

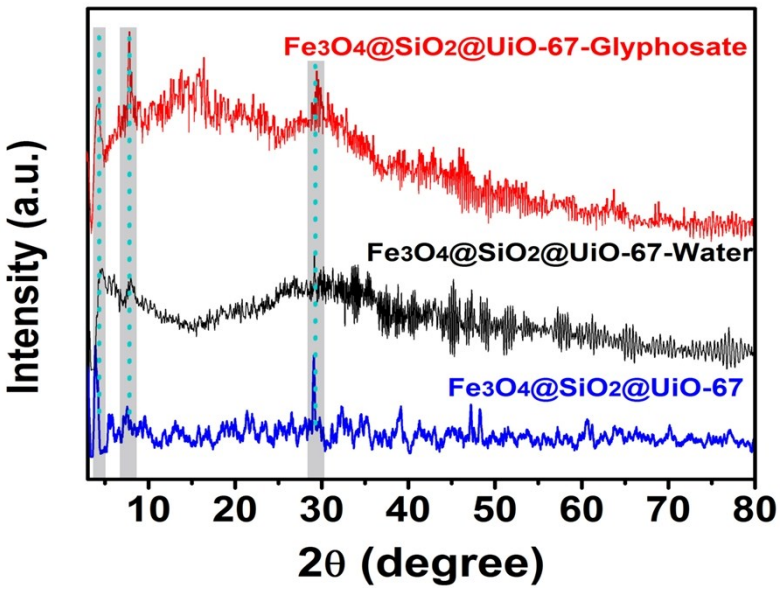

Fig. S10 XRD pattrens of Fe_3O_4@SiO_2@UiO-67 after adsorption glyphosate and dispersed in water for 48 h.

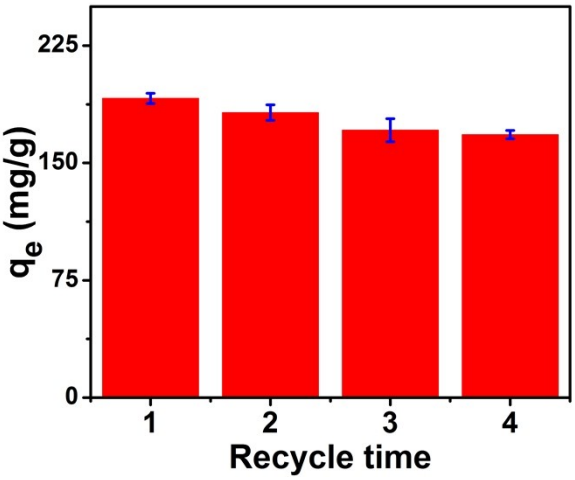

Fig. S11 Regeneration cycles on the adsorption capacity of Fe_3O_4@SiO_2@UiO-67 for glyphosate under room temperature.

Table S1 The parameters of pseudo-first-order kinetic, pseudo-second-order kinetic, and intraparticle diffusion kinetic of adsorption glyphosate.

Adsorption kinetics parameters		
Pseudo-first-order model	q_e (mg g^{-1})	140.6±10.0
	k_1 (min^{-1})	0.024±0.004
	R^2	0.7743
Pseudo-second-order model	q_e (mg g^{-1})	204.2±1.9
	k_2 (g $mg^{-1}min^{-1}$)	0.0077±0.0006
	R^2	0.9984
Intra-particle diffusion model	k_i (mg g^{-1} $min^{1/2}$)	3.72±0.70
	C (mg g^{-1})	145.05±7.21
	R^2	0.8718

Table S2 Isotherms parameters for the adsorption of glyphosate on Fe_3O_4@SiO_2@UiO-67.

Adsorption isotherms parameters		
Langmuir model	q_{max}(mg g^{-1})	256.54±5.72
	k_L(L mg^{-1})	19.21±1.36
	R^2	0.9965
Freundlich model	k_F($mg^{1-n}L^ng^{-1}$)	60.64±5.05
	n	3.26±0.25
	R^2	0.9615

Table S3 The comparison of Fe_3O_4@SiO_2@UiO-67 adsorption of glyphosate with the other reported adsorbents.

Adsorbents	q_{max} (mg/g)	ref.
$MnFe_2O_4$ – G	39.0	S8
MnO_x/Al_2O_3	116.0	S9
Alum sludge	113.6	S10
Dendro biochar	44.0	S11
Chitosan/alginate membrane	0.008	S12
Ni_2AlNO_3	172.4	S13
Fe_3O_4@SiO_2@UiO-67	256.5	This work

Table S4 Comparison of the Fe_3O_4@SiO_2@UiO-67 fluorescence sensor with other methods for determination of glyphosate.

Methods	linear range (mg/L)	R^2	LOD (mg/L)	ref
GC-MS/MS method	0.00001-0.01	0.9980	0.001	S1
Au/SAM-COOH electrode	1.69-16.90	0.9996	0.47	S2
Intramolecular Indicator Displacement Assay	0-169	Not mentioned	0.2	S3
Colorimetric method	3.38-33.80	0.9954	0.17	S4
SERS method	0-0.1	0.9910	0.0001	S5
Carbon dots sensor	0.025-2.5	0.9930	0.012	S6
Screen-printed electrodes	8.45-16.90	0.9987	0.17	S7
Fe_3O_4@SiO_2@UiO-67 sensor	0.1-40	0.9904	0.093	This work

Table S5 Recovery test and precision of the determination of glyphosate in real samples.

Samples	detected (mg/L)	spiked (mg/L)	found (mg/L)	recovery (%)	RSD (%)
tap water	Not detectable	0.5	0.486±0.02	97.3	5.3
		2.0	2.018±0.04	100.9	2.1
apple juice	Not detectable	0.5	0.453±0.01	90.6	2.3
		2.0	1.949±0.08	97.5	4.1

Reference

S1. A. Steinborn, L. Alder, B. Michalski, P. Zomer, P. Bendig, S. A. Martinez, H. G. J. Mol, T. J. Class, and N. C. Pinheiro, Determination of Glyphosate Levels in Breast Milk Samples from Germany by LC-MS/MS and GC-MS/MS, *J. Agr. Food Chem.*, 2016, **64**, 1414–1421.

S2. G. Marzari, M. V. Cappellari, G. M. Morales and F. Fungo, Electrochemiluminescent detection of glyphosate using electrodes modified with self-assembled monolayers, *Anal. Methods*, 2017, **9**, 2452-2457.

S3. T. Minami, Y. Liu, A. Akdeniz, P. Koutnik, N. A. Esipenko, R. Nishiyabu, Y. Kubo, and P. AnzenbacherJr., Intramolecular Indicator Displacement Assay for Anions: Supramolecular Sensor for Glyphosate, *J. Am. Chem. Soc.*, 2014, **136**, 11396–11401.

S4. Y. Chang, Z. Zhang, J. Hao, W. Yang, J. Tang, A simple label free colorimetric method for glyphosate detection based on the inhibition of peroxidase-like activity of Cu(Ⅱ), *Sensor Actuat, B-Chem.*, 2016, **228**, 410-415.

S5. M. Tan, Z. Hong, M. Chang, C. Liu, H. Cheng, X. JunLoh, C. Chen, C. Liao, K. V. Kong, Metal carbonyl-gold nanoparticle conjugates for highly sensitive SERS detection of organophosphorus pesticides, *Biosens. Bioelectron.*, 2017, **96**, 167-172.

S6. L. Wang, Y. Bi, J. Hou, H. Li, Y. Xu, B. Wang, H. Ding, L. Ding, Facile, green and clean one-step synthesis of carbon dots from wool: Application as a sensor for glyphosate detection based on the inner filter effect, *Talanta*, 2016, **160**, 268-275.

S7. A. Habekost, Rapid and sensitive spectroelectrochemical and electrochemical detection of glyphosate and AMPA with screen-printed electrodes, *Talanta*, 2017, **162**, 583-588.

S8. N. U. Yamaguchi, R. Bergamasco, S. Hamoudi, Magnetic $MnFe_2O_4$–graphene hybrid composite for efficient removal of glyphosate from water, *Chem. Eng. J.*, 2016, **295**, 391-402.

S9. T. Zheng, Y. Sun, Y. Lin, N. Wang, P. Wang, Study on preparation of microwave absorbing MnO_x/Al_2O_3 adsorbent and degradation of adsorbed glyphosate in MW–UV system, *Chem. Eng. J.*, 2016, **298**, 68-74.

S10. Y. S. Hu, Y. Q. Zhao, B. Sorohan, Removal of glyphosate from aqueous environment by adsorption using water industrial residual, *Desalination*, 2011, **217**, 150-156.

S11. S. S. Mayakaduwa, P. Kumarathilaka, I. Herath, M. Ahmad, M. Al-Wabel, Y. S. Ok, A. Usman, A. Abduljabbar and M. Vithanage, Equilibrium and kinetic mechanisms of woody biochar on aqueous glyphosate removal, *Chemosphere*, 2016, **144**, 2516-2521.

S12. R. T.A. Carneiro, T. B. Taketa, R. J. Gomes Neto, J. L. Oliveira, E. V. R. Campos, M. A. Moraes, C. M. G. Silva, M. M. Beppu, L. F. Fraceto, Removal of glyphosate herbicide from water using biopolymer membranes, *J. Environ. Manage.*, 2015, **151**, 353-360.

S13. A. Khenifi, Z. Derriche, C. Mousty, V. Prévot, C. Forano, Adsorption of Glyphosate and Glufosinate by Ni_2AlNO_3 layered double hydroxide, *Appl. Clay*

Sci., 2010, **47**, 362-371